GOES-17 ADVANCED BASELINE IMAGER PERFORMANCE RECOVERY SUMMARY

Joel McCorkel[1], John Van Naarden[2], Daniel Lindsey[3], Boryana Efremova[4], Monica Coakley[5], Mason Black[5], Alexander Krimchansky[1]

[1]NASA Goddard Space Flight Center, Greenbelt, MD 20771, USA
[2]Harris Corporation, Ft Wayne, IN 46818, USA
[3]NOAA/NESDIS, Fort Collins, CO 80521, USA
[4]GeoThinkTank, Washington, DC 20009, USA
[5]Massachusetts Institute of Technology, Lincoln Laboratory, Lexington, MA 02421, USA

ABSTRACT

The 17th Geostationary Operational Environmental Satellite (GOES-17) was launched on 1 March 2018. The Advanced Baseline Imager (ABI) is the primary instrument on the GOES-R series for weather and environmental monitoring. The GOES-17 ABI (flight model 2) experienced a degradation in its thermal system that limits ABI's ability to shed solar heat load. This limitation resulted in significant reduction in performance after initial turn on with only 3 of 16 spectral channels expected to be available for much of the year. A combined government/vendor team was tasked with optimizing the operation of ABI to recapture as much performance as possible. By modifying the operational configuration and sensor parameters, the team was able to regain over 97% imaging capability.

This was accomplished by taking advantage of the considerably flexible nature of ABI's design to adapt its configuration to the new reality and improve capabilities for many of ABI's subsystems. The significant differences in operational configuration, sensor parameter optimization, and algorithm optimization will be discussed as well as their impact on performance and data availability.

Index Terms— GOES, GOES-17, ABI, Advanced Baseline Imager, on-orbit sensor optimization, calibration

1. ABI INTRODUCTION

The Advanced Baseline Imager, developed by the Harris Corporation, is a multi-channel imaging radiometer used for a wide range of applications related to weather, oceans, land, climate, and hazards such as fires, volcano eruptions, and hurricanes [1]. ABI enhances the spatial resolution by four-fold compared to the previous GOES generation with 0.5-km sampling (at nadir) in the 0.64-μm channel and 1 or 2 km in the other channels. ABI employs an east-west scan mirror and motor to scan across the Earth at 1.4º per second, and a north-south mirror and motor to step swath location. Twenty-two west-east scans comprise a full disk image. These optics and large detector arrays enable ABI to observe, in 10 minutes, one full disk Earth image, two 5000×3000 km^2 Continental United States (CONUS) images, and twenty 1000×1000 km^2 mesoscale images; this represents a five-fold improvement in temporal coverage compared to the previous generation GOES imagers. ABI improves the spectral coverage by a factor of three over the previous generation of GOES-N Imagers by providing continuous Earth observation in 16 spectral bands over the 0.47-13.3 μm spectral range. A summary of the ABI spectral channels is shown in Table 1. Channels 1-3 use silicon detector arrays while the longer wave spectral channels use HgCdTe arrays. The detector array for each spectral channel employs multiple columns (3-6) of active pixels for redundancy, and hundreds of rows (332 to 1460, depending on the pixel size) to enable rapid Earth coverage.

Table 1. Advanced Baseline Imager key parameters

	Band	Center wavelength (μm)	SNR or NEdT	Nadir pixel size (km)	Band name / use
Visible/ Near Infrared	1	0.47	300	1	Blue
	2	0.64	300	0.5	Red
	3	0.86	300	1	Vegetation
	4	1.38	300	2	Cirrus
	5	1.6	300	1	Snow/ice
	6	2.2	300	2	Cloud particle size
Mid-wave Infrared	7	3.9	0.1 K	2	Shortwave window
	8	6.2	0.1 K	2	Upper-level tropospheric water vapor
	9	6.9	0.1 K	2	Mid-level tropospheric water vapor
	10	7.3	0.1 K	2	Lower-level water vapor
	11	8.4	0.1 K	2	Cloud-top-phase
Long wave Infrared	12	9.6	0.1 K	2	Ozone
	13	10.3	0.1 K	2	Clean longwave window
	14	11.2	0.1 K	2	Longwave window
	15	12.3	0.1 K	2	Dirty longwave window
	16	13.3	0.3 K	2	CO_2 longwave window

GOES-17 ABI was launched on 1 March 2018, and the first visible images acquired on 12 April 2018. A couple weeks later the team attempted to initialize the thermal system to cool the thermal focal plane to its operational temperature of 60 K; however, the two loop heat pipes, a critical link in the thermal system, did not appear to be transferring heat from the cryocooler to the radiator. Without being able to transmit its reject heat, the cryocooler rapidly reached its temperature limit requiring that it be turned off and therefore not able to cool the thermal focal plane.

The next section describes methods used to minimize the longwave focal plane temperature. Sections 3 and 4 present summaries of how we optimized sensor parameters for operation at elevated temperatures and developed extra steps in the radiometric calculation to maintain accuracy. Section 5 shows performance achieved with the combination of these efforts.

2. SPACECRAFT AND CRYOCOOLER OPERATIONS

Dozens of options were considered to reduce solar heat load on ABI, but the two with most substantial impact were implementation of semi-annual yaw flips of the GOES-17 spacecraft and optimization of cryocooler operation.

The solar beta angle has the largest impact on a seasonal scale for amount of solar intrusion into ABI that causes warming of its thermal focal plane. Optical models were used to determine the spacecraft orientation for overall minimum thermal impact; these were tested and confirmed on-orbit. Current operations will perform a yaw flip close in time to solar equinoxes to maintain optimal alignment for lowest solar loading. Figure 1 shows modeled daily maximum temperature that the longwave focal plane reaches throughout a year; the yaw flips occur at the discontinuities in March and September.

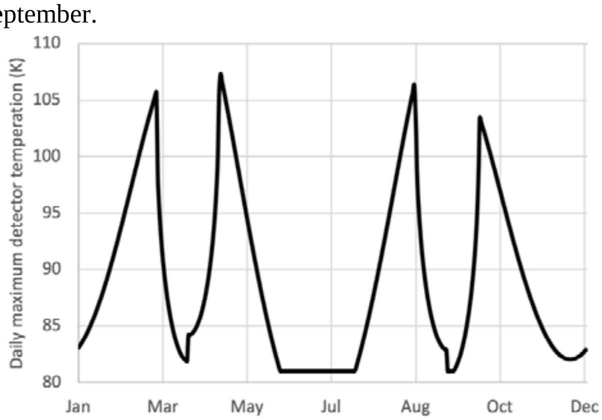

Fig 1. The daily maximum temperature of the thermal focal plane is plotted across a calendar year.

There are competing thermal processes during the eclipse season before and after equinoxes. From March equinox to the September equinox ABI is in an orientation optimized for minimizing solar energy penetrating into the aperture, but meanwhile the radiator is exposed to the sun. Then, sometime near the September equinox and going through the following March equinox, a yaw flip puts ABI in optimal orientation which points the radiator away from the sun but allows more light into the aperture depending on when the flip occurs. Work continues to optimize the timing of the yaw flips to maximize colder focal plane operation.

Cryocoolers on ABI are responsible for removing heat from the thermal focal plane, and there are two of them: primary and redundant. Rather than operating one cryocooler as prescribed for normal operations, it was found that operating both units in parallel at lower drive levels was more efficient. Since the loop heat pipes are not operating at their intended capacities, heat is not shed from the cryocooler's hot side and the reject temperature quickly reaches its limit during times of high solar load.

Initially, the cryocooler had to be turned off to avoid damage, but as it became clear that the loop heat pipe could not be revived, algorithms were developed to throttle the cryocooler drive to run as much as possible while keeping its reject temperature at a safe level. The limit of reject temperature was increased to 330 K based on studies and tests on ground-based life-test units. An example of cryocooler throttling is shown in the middle plot of Figure 2. The solar geometry overwhelms the thermal system in the ~10:00-16:00 UTC time range where the algorithm regulates the cryocooler drive to maintain a small band beneath the 330 K reject temperature limit. As the sun moves out of the ABI aperture, the reduced heat load allows the cryocooler to catchup, gradually increase its drive as directed by the algorithm, and bring the focal plane temperature down.

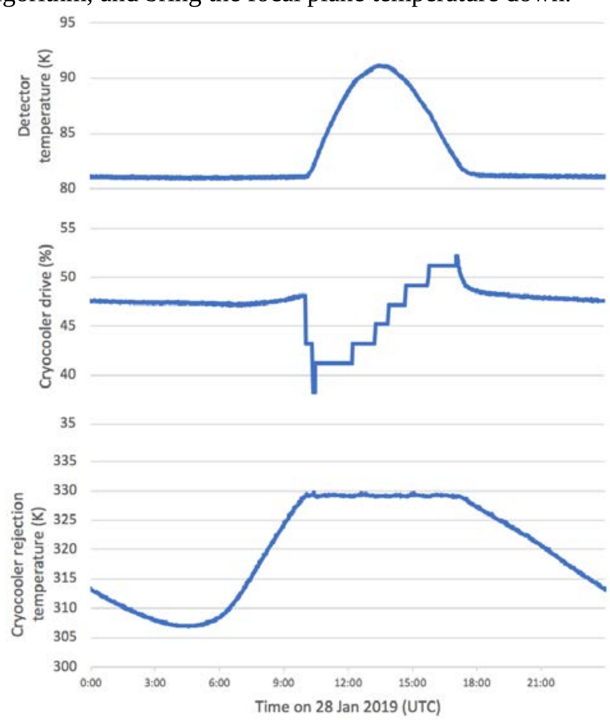

Fig 2. The cryocooler drive and rejection temperature is plotted for 28 January 2019 along with associated thermal focal plane temperature.

These operational changes minimize heat getting to the focal plane from the sun and maximize heat extraction by the cryocooler. The remaining operational change was the selection of focal plane temperature set point: too low would cause the cryocooler reject temperature to rail against its 330 K limit too quickly resulting in large temperature swings; too high would not take advantage of this optimized cooling capacity so performance would be lost. With analysis help from NOAA scientists, it was determined that 81 K set point provided optimal solution for this compromise: all the channels provide high-quality imagery while the focal plane is at its set point temperature and the unavoidable peaks in temperature are confined to certain times of the night.

While Figure 1 shows the maximum focal plane temperature each day of the year, Figure 3 shows examples of the diurnal temperature profile. Maximum solar loading occurs at local midnight when the sun is closest to ABI's boresight and the maximum focal plane temperature is observed a few hours later. The horizontal black lines indicate approximate temperatures that particular channels begin to visibly degrade and require additional calibration processing to maintain accuracy. Despite these daily peaks, the focal plane maintains its 81 K set point operation about 72 percent of the time. The next two sections describe how image quality and accuracy is improved by sensor parameter and algorithm optimization.

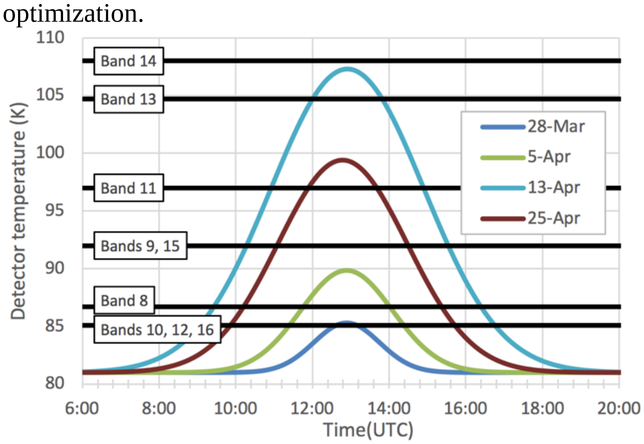

Fig 3. The infrared focal plance temperature is plotted for several days on which ABI detector temperature raises above 81 K. March 28 is an example of one of the hottest days. The maximum temperature, the peak of each colored line here, of each day is shown in Fig 1.

3. SENSOR PARAMETER OPTIMIZATION

GOES-17 ABI thermal detectors were designed to operate at around 60 K, however most of the time they will operate at 81 K with hotter periods depending on time of year and time of day. The detectors have higher dark current at these higher temperatures which means there is less dynamic range available to capture signal of Earth scenes. To compensate, gain settings were reduced by factors of 1/8 to 1/2 of their nominal values depending on channel for 81 K operation. For days when detector temperature rises above 85 K, even less dynamic range is available so gain is reduced by factors of 1/16 to 1/4. Gain reduction is achieved through combination of configurable amplifiers and integration time.

The nominal bias voltage across the detectors was optimized for operation at 60 K, but imagery was blurred with this voltage at higher-temperature operation. Bias voltage sweeps similar to ground testing were performed on-orbit to determine the optimal value for current thermal conditions. It was determined that the maximum bias available by circuit the circuit design was optimal. These new parameters dramatically improved image quality and availability.

4. CALIBRATION OPTIMIZATION

Operational changes were made to optimize the thermal system to keep the focal plane stable 72 percent of the time and sensor parameter changes were made to achieve reasonable sensitivity with these new conditions. During the remaining 28 percent of the time the focal plane experiences rising and falling temperatures, a dynamic that counters the basis of the operational radiometric calculation that depends on detector temperature stability of 0.1 K or less.

The dark current, or offset signal, and the gain changes with detector temperature. During nominal operation ABI will measure space to determine offset signal about every 30 seconds and measure the onboard blackbody to determine gain every 15 minutes. The frequency of black body measurements was increased to every five minutes. However, the offset level changes rapidly with temperature such that calculating Earth-scene radiance with a offset measurement that is a few seconds in the past causes substantial radiometric error since the 'true' offset at the time of the Earth-scene measurement has drifted due to drifting detector temperature – this effect is illustrated in Figure 4. Drifting offset also causes gain calculation inaccuracy since gain is calculated with the signal from blackbody measurement and a spacelook-derived offset measurement that occur several seconds apart from each other.

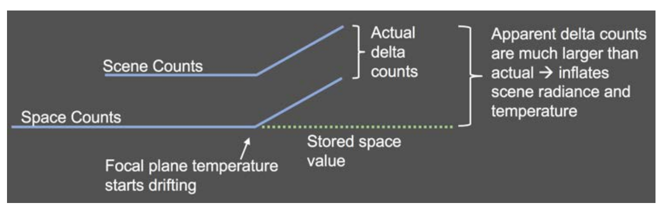

Fig 4. Illustration of offset signal drift caused by detector temperature drift that results in inaccurate radiometric calculation.

One method to reduce inaccuracy caused by drifting offset and gain is to predict the value of these quantities for the time of each Earth-scene measurement. Linear projection to predict offset levels within the 30-second frequency of space measurements is sufficient. Linear gain projection, that also accounts for predicted offset levels, is also sufficient over the five-minute blackbody measurement frequency. Both of these projections use the two most recent measurements. Figure 5 shows an example for 28 January 2019 of the correction that the predictive algorithm achieves for Band 8. The red line is the average CONUS radiance trend, resulting from the baseline processing, and the blue line is the predictive calibration result. As evident from the figure, modulations correlating with the focal plane temperature are present in the baseline-calibrated radiance, and are removed by applying predictive calibration.

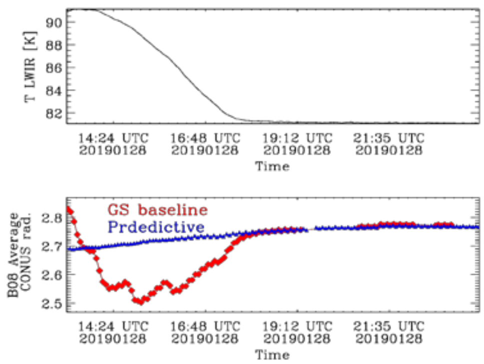

Fig 5. Predictive calibration algorithm linearly projects offset and gain to calculate accurate Earth-scene radiance. The red line shows an area-average Earth radiance calculated with the nominal radiometric algorithm and the blue line is the result using predictive algorithm.

Besides drifting offset and gain, two other features were identified and addressed to improve radiometric accuracy: memory effect after extended space look measurements and blackbody measurements in nonlinear portion of the dynamic range.

As described in the first section, ABI acquires a full disk, two continental US, and 20 mesoscale images in a 10-minute period. There are several calibration scans interspersed with the scans for these images: blackbody for gain, spacelook for offset, and star measurements for navigation. Particular spacelook and Earth scene scans that took place after the star measurements appeared to be out-of-family. Since star measurements point ABI to space for four to eight seconds, much longer than spacelook measurement for offset, it was hypothesized that extended time looking at deep space effected the signal of subsequent measurements. This effect was minimized by 1) doubling the speed of star measurements and 2) moving the scan mirrors to point at Earth for several seconds after star measurements and before Earth measurements.

During warmer focal plane periods the blackbody measurement has nonlinear response when the signal is just beneath saturation. Since gain change due to temperature change is relatively small relative to the impact of nonlinearity in this signal range, the gain is held constant when the blackbody signal is above a certain threshold.

5. IMAGING PERFORMANCE SUMMARY

Spacecraft, cryocooler, and detector temperature set point operation changes provided the best-case compromises for sensor performance: Stable operation at 81 K most of the time and varying temperature peaks throughout the year for the remaining time. Table 2 summarizes the amount of time that predictive radiometric calculation improves accuracy. Figure 6 shows the maximum correction provided by predictive algorithm throughout the year. The magnitude of the correction depends on how quickly the detector temperature is changing and dark current varies in each channel.

Table 2. Duration that predictive calibration algorithm buys back.

	Time predictive algorithm improves accuracy over 1 year (hours)	% of time predictive algorithm improves accuracy	% of time usable imagery is produced
B08 (6.2 um)	2112	24%	96%
B09 (6.9 um)	2098	24%	96%
B10 (7.3 um)	2009	23%	95%
B11 (8.4 um)	2316	26%	98%
B12 (9.6 um)	1957	22%	94%
B13 (10.3 um)	2390	27%	99%
B14 (11.2 um)	2472	28%	100%
B15 (12.3 um)	2208	25%	97%
B16 (13.3 um)	2066	24%	98%

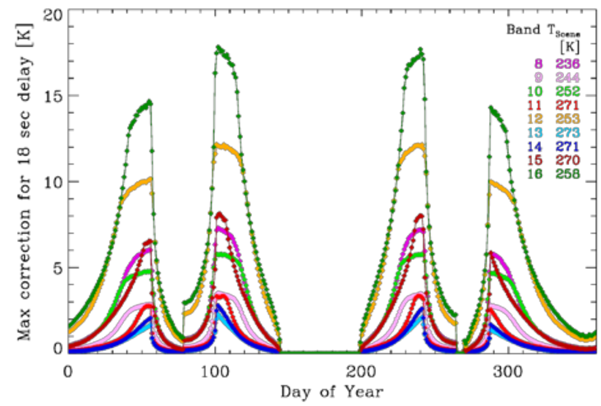

Fig. 6. Maximum correction that predictive calibration provides for each channel, at a fixed scene temperature (based on Jan 28 2019 values), as indicated in the legend, throughout a year for continental US images.

6. CONCLUSION

Performance recovery activities began once the on-orbit thermal anomaly on GOES-17 ABI was identified. Primary efforts were to 1) reduce thermal focal plane temperature as much as possible and for as long as possible; 2) optimize sensor parameters for new thermal conditions; and 3) improve calibration accuracy using predictive radiometric calculations and adjusted acquisition timelines. Through these over 97 percent of imaging capability was achieved. Mid- and long-wave infrared imagery for a few hours for some nights of the year remains unrecoverable due to elevated detector temperatures during those times.

7. REFERENCES

[1] Schmit, T.J., Griffith, P., Gunshor, M.M., Daniels, J.M., Goodman, S.J. and Lebair, W.J., 2017. A closer look at the ABI on the GOES-R series. Bulletin of the American Meteorological Society, 98(4), pp.681-698.